Least-squares (LS) deconvolution of a series of overlapping cortical auditory evoked potentials: a simulation and experimental study

Fabrice Bardy MClin Aud[1,2,3]

Bram Van Dun PhD[1,3]

Harvey Dillon PhD[1,3]

Robert Cowan PhD[1]

[1] HEARing Co-operative Research Centre, Australia

[2] Department of Linguistics, Macquarie University, NSW, Australia.

[3] National Acoustic Laboratories, NSW, Australia

Correspondence to:

Fabrice Bardy

Australian Hearing Hub

16 University Avenue

Macquarie University NSW 2109 Australia

P +61 2 94 12 68 14

F +61 2 94 12 67 69

Email: Fabrice.Bardy@nal.gov.au

Highlights

- The LS deconvolution enables us to disentangle a series of overlapping cortical auditory evoked potentials (CAEPs) recorded under high presentation rates in response to different stimuli.

- The signal-to-noise ratio (SNR) achieved at high presentation rates is lower compared to conditions where CAEPs are not overlapping.

- The use of the LS deconvolution allows us to understand inhibitory mechanism of the brain under fast auditory stimulation.

Key words

- Cortical auditory evoked potentials

- Least-squares deconvolution

- Multiple overlapping responses

- Low-jittering

- SNR

Abstract:

Objective: To evaluate the viability of disentangling a series of overlapping "cortical auditory evoked potentials" (CAEPs) elicited by different stimuli using least-squares (LS) deconvolution, and to assess the adaptation of CAEPs for different stimulus onset-asynchronies (SOAs).

Design: Optimal aperiodic stimulus sequences were designed by controlling the condition number (CN) of matrices associated with the LS deconvolution technique. First, theoretical considerations of LS deconvolution were assessed in simulations in which multiple artificial overlapping responses were recovered. Second, biological CAEPs were recorded in response to continuously repeated stimulus trains containing 6 different tone-bursts with frequencies 8, 4, 2, 1, 0.5, 0.25 kHz separated by SOAs jittered around 150 (120-185), 250 (220-285) and 650 (620-685) ms. The control condition had a fixed SOA of 1175 ms. In a second condition, using the same SOAs, trains of 6 stimuli were separated by a silence gap of 1600 ms. Twenty-four adults with normal hearing (<20 dB HL) were assessed.

Results: Results showed disentangling of a series of overlapping responses using LS deconvolution on simulated waveforms as well as on real EEG data. The use of rapid presentation and LS deconvolution did not however, allow the recovered CAEPs to have a higher signal-to-noise ratio (SNR) than for slowly presented stimuli.

Conclusion: The LS deconvolution technique enables the analysis of a series of overlapping responses in EEG.

Significance: LS deconvolution is a useful technique for the study of adaptation mechanisms of CAEPs for closely spaced stimuli whose characteristics change from stimulus to stimulus. High-rate presentation is necessary to develop an understanding of how the auditory system encodes natural speech or other intrinsically high-rate stimuli.

1. Introduction

Cortical auditory evoked potentials (CAEPs) represent time-locked neuronal activity generated in the auditory cortex in response to sound stimuli. This objective measurement is increasingly used by audiologists in clinical practice to evaluate the audibility of sound presented via hearing aid amplification for babies or toddlers, or for adults who are not able to participate in conventional hearing testing (Billings et al, 2012, Rance et al, 2002, Van Dun et al, 2012). Three main advantages of CAEPs over other non-invasive electrophysiological measurements used to assess hearing can be identified. First, these potentials can be easily recorded while the subject is awake. Second, when compared to auditory brainstem responses where the stimuli used are extremely short (i.e. clicks stimuli), CAEPs can be measured using stimuli lasting up to hundreds of milliseconds. The stimuli are therefore long enough in duration to be captured and processed by a hearing aid in a state similar to the state it is in in real-life speech signal (Souza and Tremblay, 2006). Third, the morphology of the waveforms, including such aspects as latency, correlate well with speech perception scores and functional measures of hearing ability such as the parents' evaluation of oral performance of children (PEACH) (Golding et al, 2007) or the infant-toddler meaningful auditory integration scale (IT-MAIS) (Sharma et al, 2007).

Parameters for recording CAEPs recommended for clinical use include a stimulus onset-asynchrony (SOA) of 1 to 2 seconds (Cone and Whitaker, 2013, Golding et al, 2006, Van Dun et al, 2012). This criterion is used to both maximize response amplitudes and avoid overlap of multiple components of the cortical response. Taking into account that CAEPs elicited by an acoustic stimulus can last more than 300 ms in adults, and even longer in infants, responses will overlap significantly when SOAs are in the range of only hundreds of milliseconds. The use of SOAs shorter than the response length leads to difficulties in interpreting the waveform morphology of overlapping responses (Sable et al, 2004, Sussman et al, 2008). However, understanding how the auditory cortex encodes temporal acoustic information presented at rates similar to syllable rate in speech is of great interest. Yet few

studies have been conducted using short SOAs to record CAEPs, mainly because of the lack of

flexible methods to distinguish between overlapping responses. Consequently, little is known about

the adaptation characteristics and waveform morphologies under such conditions. Further research

in this area may provide insights into the underlying mechanisms of more complex tasks, such as

speech encoding in the normal or impaired auditory system.

Although mathematical deconvolution techniques have been described formerly (Delgado and

Ozdamar, 2004, Eysholdt and Schreiner, 1982, Jewett et al, 2004), there has been a recent increased

interest in analysis of multiple (auditory) evoked responses overlapping in time (Bardy et al, 2014a,

Valderrama et al, 2012, Wang et al, 2013b). The application of powerful mathematical techniques to

disentangle and recover transient responses to stimuli presented at very rapid rates is opening new

doors in electrophysiological research. A major advantage of these new techniques, such as least-

squares (LS) deconvolution (Bardy et al, 2014a), is the ability to apply the deconvolution to

sequences containing multiple types of interleaved stimuli. Interleaving different stimuli is

particularly interesting to prevent the adaptation of the CAEP often seen in paradigms involving the

response to a single stimulus presented at high rates (Herrmann et al, 2013). Moreover, presenting

multiple stimuli closely spaced together in time allows the design of stimulus sequences which are

more closely related to the natural sound environment.

One theoretical requirement for deconvolution is the presence of varying SOAs between different

stimuli in a sequence. This is referred to as jitter. If no jitter is present, a solution for the

deconvolution problem currently does not exist. On the other hand, it is important to keep the

amount of jitter to a minimum in order to limit the variability of the response, which is affected by

the SOA from the previous stimulus. This issue is especially present when recording CAEPs.

Mathematically, the arrangement of timing intervals of the stimulus sequence has been shown to be

of critical importance to control the excessive post-deconvolution noise, also called "numerical

error" in this study, introduced by the inversion necessary to deconvolve the responses in the signal.

A practical method has been proposed by (Bardy et al, 2014a) that allows the selection of sequences, consisting of multiple stimuli to sufficiently reconstruct overlapping responses, by searching for a minimum condition number (CN). The CN of the sequence is irrelevant when deconvolving noiseless data, but it is highly relevant in noisy conditions, which is inevitable when recording EEG data.

Only a handful of studies have investigated the overlap of cortical responses using the Adjar deconvolution technique level 1 under a high-jitter condition (Budd and Michie, 1994, Sable et al, 2004, Wang et al, 2008a). Additional studies have investigated the overlap of two cortical responses using a paired paradigm (Bardy et al, 2014b, Fox et al, 2010). These studies reported an increase of the CAEP amplitude for SOAs shorter than 400 ms. When presenting at high-rates, the increased number of responses has the potential to reduce the noise proportionally to the square root of the number of trials. The SNR, and consequently the detection process, have the potential to improve depending on the influence of the stimulation rate on the response amplitude and the amount of numerical error introduced by the LS deconvolution. Any technique allowing a potential reduction in testing time, which is still relatively long using conventional methods, is in our view worth investigating. However, other studies using high-rate stimulation sequences did not report the SNR/efficiency relationship for CAEPs (Budd and Michie, 1994, Sable et al, 2004). In addition, we are not aware of any studies reporting on cortical response morphology using a stimulus sequence containing different stimuli, using high-rate stimulation and under low-jitter condition.

In this study, we investigated four aspects of experimental paradigm using high-rate stimulation to record CAEPs. First, using simulations, we examined the numerical noise introduced by the LS deconvolution recovery sequence, depending on the stimulation rate. Second, using experimental data, we investigated the ability of LS deconvolution to disentangle series of overlapping CAEPs, and characterize the waveform morphology of the response. Third, we measured the adaptation characteristics of cortical auditory evoked responses when presented rapidly. This measure provided

an estimation of the CAEP amplitude reduction or increase associated with increasing stimulus rates. Finally, measures of signal and noise power allowed a systematic investigation of signal-to-noise ratio (SNR) of the response to different stimulus sequences composed of short SOAs. These studies extend the work previously reported in (Bardy et al, 2014a, Bardy et al, 2014b) by including longer trains of diverse stimuli, with and without intervening longer gaps.

2. Method

To evaluate the utility of the LS deconvolution technique in separating multiple overlapping responses, both simulated and experimental data were analyzed using similar stimulus sequences. Previous studies have shown that when applying the deconvolution technique, there is a risk of introducing numerical error in noisy conditions (Ozdamar and Bohorquez, 2006, Wang et al, 2013b). For this reason, stimulus sequences were optimized to minimize the numerical error introduced by the LS deconvolution. This error is a characteristic of the deconvolution technique which is inevitable but predictable and controllable (Bardy et al, 2014a).

2.1 Stimulus sequences

As shown in Figure 1, a stimulus sequence was composed of an integer number of subsequences. All the subsequences were composed of six stimulus trains, each of which contained six tone-burst stimuli. The six tone-bursts were always presented in the same order and each tone-burst potentially generated a different CAEP (see Section 4 for the parameters used in real-life data collection).

2.1.1 Sequence characteristics

Three conditions were tested, comprising a total of seven stimulus sequences (see Figure 1 and Table 1):

a) In the first condition, three different SOAs jittered around 150, 250 or 650 ms were investigated. Throughout the paper, we will refer to these as sequences S1, S2 and S3 respectively.

b) In the second condition, the SOA was constant and equal to 1175 ms. This measure corresponds to a SOA conventionally used in clinical practice for CAEP recording (sequence S4).

c) In the third condition, a constant inter-train interval of 1600 ms (referred to as GAP) was separating each stimulus train. The SOAs between the stimuli of the train were jittered around 150, 250 or 650 ms, similar to the first condition, and as shown in Figure 1. Here, we will refer to sequences S5, S6 and S7 respectively.

The measurement time for each sequence was kept relatively constant (between 8.24 and 9.14 minutes) which results in for more presentations of the short SOA ranges, as shown in Table 1. Each sequence was made of an integer number of subsequences, each which contained 36 stimuli. It was therefore not possible to create sequences of exactly the same duration.

2.1.2 Generation of specific sequences to allow optimal deconvolution

When using SOAs with shorter duration that the length of the cortical response, overlap between different responses is inevitable. Hence, a technique is required to 'deconvolve', or disentangle, these overlapping responses. The technique used in this manuscript is based on a combination of convolution theory and mean square error minimization (Bardy et al, 2014a). The latter approach is introduced to minimize the residual error between the reconstructed response and the (unknown) original response in the time domain.

A prerequisite for the deconvolution approach is that the repetition period of the stimuli in the sequence exhibits sufficient jitter. The characteristics of this jitter (distribution of SOAs in the stimulus sequence) influences the quality of the recovery process. From a purely mathematical point

of view, a large amount of jitter will minimize numerical noise in the recovered waveforms. On the other hand, it is well documented that the cortical response adapts in morphology and amplitude depending on the time interlude from the preceding stimulus (Sussman et al, 2008). Hence, it is important to minimize the amount of jitter to reduce any change in the response, while keeping the jitter large enough, such that the inversion process of the deconvolution technique is not too numerically unstable.

To optimize the sequences for this study, a method described in Bardy et al (2014a) was used by minimizing the condition numbers (CNs) of the matrices involved in the deconvolution. Based on simulations using cortical response parameters (Bardy et al, 2014a), a trade off value of 65 ms of jitter normally distributed around the SOA of each range was used. This jitter range allows a reasonably low CN, as well as a minimum change of the morphology of the response in one jitter range, quantified using an intra-class correlation coefficient (ICC). Additionally, an aperiodic model of the deconvolution was implemented in which each subsequence has a different SOA randomization (see Figure 1). The use of such a technique allows a further reduction of the CN of a full stimulus sequence. A detailed description of this method is provided in Bardy et al (2014a). A further benefit of using subsequences is that for each one a corresponding response can be recovered and used for the statistical detection of the waveform and estimation of the noise, as described in Section 3.2 and represented in Figure 2.

3. Simulations

In this section we report the results obtained with simulations, which will then be compared to experimental data in Section 4. The main goal of the simulations was to test the ability of the LS deconvolution to reliably unwrap multiple overlapping cortical responses. Simulations provide a controlled validation test to predict the impact of numerical operations on the quality of the deconvolution process. A schematic representation of the different phases of the simulation is shown in Figure 2.

3.1 Methods

To be able to compare simulated data with real data, a synthesized EEG data set was generated using waveforms which mimic the waveform morphology of EEG responses evoked by auditory stimuli (see Figure 2). Different waveform morphologies with a length of 400 ms were used to simulate responses for each of the 6 tone-burst stimuli R1 to R6 (see Figure 2). Although there is evidence for a change of amplitude of the CAEP with SOA (Sussman et al, 2008, Yamashiro et al, 2011), the magnitudes of the responses R1 to R6 were kept constant. Simulations were conducted in noisy conditions by adding a noise component (3-15 Hz band-pass filtered zero-mean Gaussian noise) on top of the convolution of the six different stimuli with known timing sequences, as described in Section 2.1.1. The main aim was to mimic the presence of internal and external noise to realistically simulate electrophysiological recordings.

Condition numbers of the sequences are given in Table 1. A CN equal to 1 indicates the absence of overlap. CN increases with a decrease of SOA, and decreases when a gap of 1600 ms is introduced (see Figure 1). As stated previously, the CN is positively related with the numerical error introduced through deconvolution in noisy situations.

In the last step of the simulations, convolved responses were recovered using LS deconvolution to produce waveforms D1 to D6. For each sequence arrangement, the quality of response recovery was evaluated using the intra-class correlation coefficient (ICC), which is a measure of similarity between the input responses R1 to R6 and the deconvolved or "recovered" responses D1 to D6 respectively at the output of the simulation. A specific ICC case, defined as an 'absolute agreement definition' by McGraw and Wong (1996) was used for this purpose.

3.2 Signal and Noise Power Calculation

The 'signal + noise' power was expressed as the mean of the squared samples within a window of 250 ms beginning at stimulus-onset. For experimental data, the benefit of using a mean squared

value when compared to squared (peak-to-peak) amplitudes is that it does not make any assumptions about the morphology of the waveform, which is different for each SOA condition. The residual noise power in the recovered waveform was calculated using two methods. Method 1 estimated residual noise power before deconvolution (see Figure 2) by calculating the mean of the squared data samples of a particular recording, divided by the number of presentations of a particular stimulus. When a signal was present, the estimation of the residual background noise was conducted with the assumption that the power of the signal would be negligible in comparison to the noise power present in the recording. In Method 2, the residual noise power was estimated using the deconvolved responses from each subsequence. The residual noise was then calculated as the mean of the sample variances at each time point within a 250 ms window starting at onset and divided by the number of subsequences. The number of subsequences is equal to the total number of stimuli in one sequence divided by the number of tone-bursts in one subsequence (which is equal to 36 in this experiment, as clarified in Figure 1). Comparing the two methods of calculation, the second method was calculated after deconvolution, whereas the first method was calculated before deconvolution using a more 'conventional' noise calculation which allows an estimation of the numerical error introduced by the deconvolution. The signal to noise ratio (SNR) expressed in decibels (dB) was then calculated as follows

$$SNR(dB) = 10 \cdot \text{LOG}_{10}\left(\frac{\text{Power}_{Signal} - \text{Power}_{Noise}}{\text{Power}_{Noise}}\right)$$

where noise power was estimated using either method 1 or 2.

3.3 Results

In this section, results are reported for the simulations described as sequences S1-S7. Figure 3 shows the 6 original waveforms used at the input of the simulation (thick line), superimposed on the recovered responses at the output of the simulation, in the case of overlapping responses (bottom row) or in the absence of overlapping responses (upper row). Reporting is guided by Figure 4, which

allows comparison of the input (before deconvolution) and the output (after deconvolution) of the simulations in terms of signal and noise power as well as SNR and quality of response recovery.

3.3.1 Quality of response recovery

The quality of response recovery is measured by the intra-class correlation coefficient (ICC), averaged over all 6 artificial responses (Figure 4.D). The simulations show that ICC values obtained when using LS deconvolution in sequences S1, S2, S5 and S6 are comparable to sequences S3, S4 and S7, where standard averaging techniques was used to recover the responses. As is evident, the deconvolution technique enabled overlapping responses to be unwrapped, even in the case of extensive temporal overlap in a data set with multiple different events in noisy conditions.

3.3.2 Signal and noise power in the recovered response

Figure 4. A shows that the estimated signal + noise power calculated at the output (after deconvolution) is generally larger compared to the input signal (before deconvolution) for simulation. As described in Section 3.2, noise calculation method 1 is calculated prior to deconvolution, and hence the numerical error introduced by the deconvolution is not taken into account in this method of calculation. Conversely, the second noise calculation method is based on the waveforms recovered after deconvolution, and includes the effects of both the artificial noise introduced at the input of the simulation as well as the numerical error introduced by the deconvolution. The difference in the simulation between the noise values based on the two calculation methods represented in figure 4.B, can be viewed as the numerical error introduced by the deconvolution. For sequences S3, S4 and S7, where the CN is equal to 1 (i.e. no overlap of responses), the two noise values match, which validates the two calculation methods. The results of the simulation show that the value of noise presented in the response after deconvolution is related to both the CN of the sequence and the number of subsequences in one sequence. Comparing noise values between the two calculation methods for sequence S1 and S5 (e.g., comprising a similar CN

but different number of subsequences) allows us to investigate the averaging property when using the deconvolution. Conversely, comparing sequence S3 with S6 (i.e. different CN, similar number of epochs averaged) allows us to investigate the impact of the CN on the amount of numerical error introduced in the average response.

3.3.3 SNR

The SNR values reported in Figure 4.C are based on the signal and noise measures in Figure 4.A and B. As indicated by the constant signal power of responses for any sequence of the experiment (see Figure 4.A), the simulations incorporate an ideal, but unrealistic, situation in which there is no decrease of the waveform amplitude with increasing presentation rates (i.e. decreasing SOA), normally caused by adaptation to repeated stimuli. However, by excluding the adaptation component in this simulation, in which testing time was kept relatively constant between each sequence, the maximum efficiency improvement achievable using fast rate presentation can be calculated. The SNR results presented in Figure 4.C show that the potential SNR gain for short SOA conditions with increasing the number of stimulus presentations, when compared to reference sequence S4 (SOA = 1175 ms), is partially offset by the introduction of numerical error by the deconvolution technique. This observation still holds after optimization of the stimuli sequence by using the lowest CN available for a specific set of parameters. In the absence of numerical error, Figure 4.C shows that an SNR improvement of 8.3 dB could be achieved by decreasing SOA from a constant 1175ms (sequence S4) to a jittered condition around 150 ms (sequence S1). However, the real SNR improvement is only 2.4 dB because of the numerical error introduced by the deconvolution. Compared to the control condition (sequence S4), a maximum SNR of 4 dB improvement was obtained for sequence S2 (SOA~250 ms).

3.3.4 Conclusion

In conclusion, these simulations confirm that the deconvolution technique can be effectively used to unwrap multiple overlapping responses, based on the high ICCs in Figure 4.D. However, LS deconvolution technique is significantly limited in its ability to increase efficiency because of the numerical error introduced during the unwrapping process.

4. Real-life data

Subsequent to simulations to verify the reconstruction capabilities of the LS deconvolution technique applied to a series of consecutive overlapping responses, physiological data were collected and analyzed to evaluate the effect of rapid presentation on actual responses measured from the brain.

4.1 Methods

4.1.1 Subjects

Twenty-four adults volunteers were recruited, comprising 5 men and 19 women, with a mean age of 28.2 yr (SD=3.6 yr). All subjects had auditory thresholds within normal limits bilaterally (<20dB HL) for octave audiometric frequencies as confirmed by audiological evaluation conducted prior to the electrophysiological testing. This study was conducted under the ethical approval and oversight of the Australian Hearing Human Research Ethics Committee and the Macquarie University Ethics Review Committee. All participants signed forms that acknowledged their informed consent.

4.1.2 Stimuli

Each stimulus train consisted of six tone-burst stimuli, binaurally presented through ER-3A insert phones, at a presentation level of 55 dB HL from high to low frequency with frequencies of 8, 4, 2, 1, 0.5, and 0.25 kHz. Changing the stimulus frequency from high to low was found to be the best strategy to allow larger amplitude of the CAEPs, based on two sets of experimental data using paired stimuli (Bardy et al, 2014b) and pilot data on a series of stimuli. This pattern is similar to the upward

spread of masking phenomenon (Oxenham and Plack, 1998). The stimuli were 50 ms in duration to maximize CAEP amplitudes (Onishi and Davis, 1968, Stapells, 2002) with a 10 ms rise-fall time to minimize spectral splatter. Stimuli were acoustically calibrated in an HA-2, 2-cc coupler using a Brüel & Kjaer 4230 sound level meter.

4.1.3 Apparatus

Three gold-plated cup electrodes were attached at the vertex, left mastoid, and forehead (ground) with impedances less than 5 kΩ. A Neuroscan®Synamps2 4.3 version (Compumedics) was used to record the CAEPs. All EEG channels were amplified with a gain of 2010, digitized at a sampling rate of 1000 Hz, and online bandpass filtered between 0.1 and 30 Hz. All epoched files were exported to MATLAB for off-line processing. The signal processing on the raw EEG files was partly conducted using EEGLAB (Delorme and Makeig, 2003), an open source toolbox designed to be used in a MATLAB environment.

The artefact rejection was conducted in the deconvolution algorithm where samples of the continuous EEG signal in excess of $\pm 45\mu V$ were excluded. The artefact rejection impacted the construction of the matrix involved in the deconvolution. Consequently, the CN in experimental data after artefact rejection reported in table 1 was always slightly larger than the CN in simulation. However, the similarity of CN values obtained for simulation and experimental data indicated that the artefact procedure was not disturbing the characteristic of the sequences too severely, so a satisfactory reconstruction was achieved. The EEG files were offline bandpass filtered between 3 and 15 Hz using a zero-phase filter. For deconvolution, the response length was assumed to be 400 ms starting from stimulus onset. The deconvolution was first applied using a response length of 500 ms including a 100 ms pre-stimulus baseline. However, increasing the length of the response impacted on the CN of the sequence. As the baseline was not providing extra information about the morphology of the response, we therefore analyzed data without a baseline period in the deconvolution to improve the CN associated with deconvolution of the response.

4.1.4 Procedure

The data recording lasted approximately 2 hours and was conducted in a sound-attenuated test booth at the National Acoustic Laboratories. CAEPs were recorded with the subject sitting in a comfortable armchair watching a sub-titled DVD with the sound turned off. The subjects were given a 3 minute break at the end of each sequence.

4.1.5 Data analysis

First, data analysis consisted of a morphology description of the CAEPs for the different frequency responses of each sequence. Second, statistical analysis was performed using two-way repeated measures ANOVAs. The effect of the 7 sequences (which vary in their SOA arrangement), and the 6 stimulus frequencies on the cortical response were analyzed in a 7 x 6 design for signal power, noise power and SNR. Planned comparisons were used to investigate the effect of the inter-train interval of 1600 ms by contrasting sequences S1, S2, S3 to S5, S6 and S7 respectively.

4.2 Results

4.2.1 Morphology description

The grand population averages of the deconvolved CAEPs are illustrated in Figure 5, and allow a comparison of the morphology of the response for gradually decreasing SOAs. The main cortical components P1, N1 and P2, in the range 0 to 250 ms, can clearly be identified in the grand averages. The adaptation of the response with SOA decrease is smaller in sequences in which there is the presence of a gap of 1600ms between stimulus trains (see Figure 5.B). This outcome verifies that CAEP elicited using SOA, as short as hundreds of millisecond, can be unwrapped using the LS-deconvolution, and supports the hypothesis that the CAEP amplitude is highly sensitive to the presentation rate.

4.2.2 Signal power analysis

In our data, the variance across participants of the signal power is not homogenous across SOA conditions. This was also observed by Zacharias et al (2011). In both studies, the standard deviation (SD) is close to linearly related to the arithmetic mean response power. In these cases, when the signal power of evoked responses from different SOA conditions differs largely with a linear scaling factor, a log transform can be applied to the signal power to make the variance less dependent on the mean (Figure 6.A).

Statistical analysis confirmed a significant main effect of SOA ($F(6,138)=68.325$; $p<0.0001$) and stimulus frequency ($F(5,115) = 24.70$; $p < 0.00001$; $\varepsilon = 0.72$) on the signal power of the cortical response (Figure 6.A and Figure 7). Figure 6A shows a decrease of the signal power with decreasing SOA for both gap (sequences S5, S6 and S7) or no-gap conditions (sequences S1, S2, S3 and S4).

There was a gradual increase in the signal power of the response from high frequencies to low frequencies with maximum amplitude for the 500 Hz tone-burst stimulus. Lastly, a planned comparison shows a significant increase of the cortical amplitude when each train was separated by gap of 1600 ms ($F(1,23)=259.12$; $p<0.0001$), as shown in Figure 7. The first stimulus of the train (8000 Hz tone-burst) in the gap condition has larger amplitude when compared to the no-gap condition which is of low amplitude (see Figure 5). The amplitude increase of the response to the 8000 Hz tone-burst is expected in line with a long recovery time after the gap of 1600ms.

The cortical responses were above noise floor in every tested condition except for the 8 kHz and 4 kHz frequencies in the no-gap condition with the ~150ms and ~250ms SOAs. For these 4 conditions, where the SNRs are smaller than 0 dB, morphology accuracy of the recovered response is questionable and conclusions should not be drawn.

4.2.3 Noise power analysis

Grand averages of log-transformed noise power, collapsed over all stimulus frequencies for each sequence, are shown in Figure 6.B, together with corresponding inter-participant standard deviations. Similar to the simulation data in Section 3, noise was calculated before and after

deconvolution, allowing measurement of the impact of the deconvolution on the amount of "numerical error" introduced in the response. A similar trend as in the simulations is observable when the CN is larger than 1. Figure 6.B shows the limited ability of the deconvolution to reduce noise in the recording by increasing the stimulus presentation rate. The noise calculation based on the signal before deconvolution shows what the residual noise would be if we were able to use normal averaging, whereas the noise estimation after deconvolution (see Section 3.2) provides an indication of the residual noise after deconvolution of the signal. As shown, the noise level after deconvolution for sequences S1 and S2 (with SOAs of ~150 and ~ 250 ms), in which a larger number of presentations is possible in the same time frame, is not improved when compared to sequence S3 in which there was no overlap.

Of interest, the noise power in sequence S5 (SOAs of ~150 ms +GAP) was even larger than the control condition (i.e. sequence S4 SOA =1175ms), demonstrating the limitation of deconvolution to significantly reduce the noise contained in the averaged response in paradigms using fast presentation rates.

4.2.3 SNR analysis

SNRs calculated from the waveforms before and after deconvolution are shown in Figure 6.C. The top trace illustrates SNR values in the ideal case with the deconvolution not introducing additional noise into the data and hence with the residual noise power decreasing with the number of stimuli in the sequence. In this condition, no significant difference across the seven different sequences was observed. This result suggests that the benefit of increasing the stimulation rate and thereby decreasing residual noise (in certain conditions) is almost exactly matched by the decrease of cortical response amplitude. The lower trace displays results in which the noise introduced by the deconvolution is taken into account. Planned comparisons show a significantly lower SNR for the sequences using a high presentation rate (p<0.001). Therefore, when considering adaptation of the

response using high presentation rates and the introduction of numerical error by the deconvolution technique, the LS deconvolution is not able to improve SNRs of cortical responses.

5. Discussion

The overlap of cortical auditory responses evoked by temporally closely spaced stimuli is a problem when interpreting results. In this study, we first validated through simulation the deconvolution of low-jittered sequences containing multiple stimuli and various SOAs. An evaluation of the numerical error introduced by the LS deconvolution technique, as well as the efficiency of the different sequences was reported. Secondly, experimental CAEP data in response to tone-burst stimuli of varying frequencies were investigated and a proof of concept was provided that this method could improve the interpretation of data recorded at high-rates presentation. Moreover, the use of LS deconvolution allowed the investigation of the adaptation of the transient auditory cortical response (i.e. CAEP) to rapidly presented stimuli (i.e. up to ~6 Hz). The adaptation was characterized by a large amplitude reduction of the CAEPs for the short SOA conditions (see Figure 5 and 6.A).

5.1 Simulations

In order to check the new algorithm in a multi-stimulus paradigm, LS deconvolution was performed on simulated data. The high waveform recovery quality measured using the ICC between input and output responses of the simulation proved the general feasibility of the deconvolution of multiple overlapping responses in noisy conditions. An important step of the LS deconvolution was the optimization of the sequences to minimize the numerical error introduced by the deconvolution in a low-jitter condition. Multiple parameters can affect the deconvolution process, such as the amount of jitter in the stimulus sequence, the sampling rate, the length of the deconvolved response, and the amount of overlap of the response. All these parameters influence the effectiveness of the deconvolution, specifically in noisy environments as already demonstrated (Bardy et al, 2014a, Wang et al, 2013a).

There is growing interest in designing optimal stimulus sequences for deconvolution with the purpose of minimizing the numerical error introduction by the technique. Valderrama et al (2012) proposed to generate sequences using random SOA arrangements without any consideration of condition number (CN). Another recent study conducted by Wang et al (2013b) suggested a 'regularization' of the transformation matrix to prevent it from being ill-conditioned. They illustrated that the regularization problem is complex and difficult to implement. Conversely, and as introduced by Bardy et al (2014a), our goal was to maximize deconvolution accuracy by selecting sequences with the lowest CN for each set of parameters. The CN provides a sensitivity measure of numerical instability. A small condition number of the matrix that gets inverted during deconvolution is essential for an accurate response recovery in noisy conditions. In this study, the stimulus sequences were composed of multiple subsequences as illustrated in Figure 1. Such an aperiodic sequence design was used because it better attenuates noise when compared to periodic deconvolution that amplifies the noise in certain frequencies (Mou-yan and Unbehauen, 1995).

The first characteristic of the LS deconvolution is the ability to design low-jittered sequences to investigate high-rate stimulation. A low variation of the jitter in the stimulus sequence results in a less variable cortical response. A stable response is a prerequisite for the deconvolution to work, as the waveform evoked to each stimulus in a particular sequence is assumed to be shape-invariant in one jitter range. The second characteristic of the LS deconvolution is the flexibility to design sequences containing different stimuli. It is particularly beneficial compared to continuous loop averaging deconvolution (CLAD) or quasi-periodic sequence deconvolution (QSD) where design is only possible for sequences containing a single unique stimulus (Delgado and Ozdamar, 2004, Jewett et al, 2004).

In general, the CN of a sequence increases as the SOA decreases because the responses overlap more severely. Consequently, sequence S1 (SOA jittered around 150 ms) had the largest CN. The CN decreased slightly in the presence of a gap (i.e. sequences S5 and S6 compared to sequences S1 and

S2) and became equal to 1.0 in the absence of overlap (i.e. sequences S3, S4 and S7). The artificial data used in the simulations had a noise component with a spectral content similar to the one of a cortical response. Investigating the effect of noise in the data is important in order to evaluate the ability of the deconvolution to speed up recording. Previous research by Bardy et al (2014a) showed that the signal averaging properties are conserved using deconvolution and that the noise amplitude present in the recording can be lowered by the square root of the number of stimulus presentations. Additionally, the present results showed that the amount of numerical error introduced by the deconvolution is correlated with the CN of the matrix involved with the deconvolution. An estimation of the numerical error power was obtained by comparing noise values taken after deconvolution to the noise values that would be expected in the case of normal averaging (see Figure 4.B).

The results of the simulations in Section 3 showed that even after sequence optimization, and in noisy backgrounds comparable to EEG recordings, only a limited SNR improvement is possible as compared to sequences having a lower presentation rate with no overlapping responses and a CN equal to 1 (Figure 4.C). Consequently, our simulations showed the limitation of low-jittered sequences to decrease testing time, especially if we consider that physiological responses adapt and decrease in amplitude for high presentation rates. This observation is in agreement with previous findings of Wang et al (2008b) who showed, using simulations, the limitation of low-jittered sequences, such as the CLAD technique for testing time reduction (Wang et al, 2008b). Experimental results obtained for real-life CAEPs discussed in the following section provide further information about the amplitude decrease and response adaptation associated with a presentation rate increase. Lastly, the simulations showed similar ICC values for the responses recovered with conventional averaging and LS deconvolution. It is demonstrated here that the LS deconvolution can reliably recover severely overlapping CAEPs, when assuming an additive system and the constant response morphology in a fixed jitter range. It demonstrates the applicability and potential of the

deconvolution to better estimate the true CAEP in case of high presentation rates and overlapping responses.

5.2 Experimental data

The experimental part of this study was designed to investigate the effect of fast stimulation rates on CAEPs. Such experimental conditions have not been investigated previously to our knowledge. Fast stimulation rates lead to overlapping of the response waveforms and modification of the morphology of succeeding response by its preceding stimuli, therefore causing difficulties with the interpretation of response morphology. The LS deconvolution technique allows each individual response waveform to be extracted, together with considerable flexibility when designing stimulus sequences. The stimulus sequences were characterized by low-jittered conditions and the inclusion of multiple stimuli.

This study allowed an initial investigation of response adaptation originating from the auditory cortex elicited by rapidly presented auditory stimuli. The results showed that response adaptation depended both on the SOAs between the tone-burst of the train as well as the presence or absence of a longer gap (1600 ms) between each train of stimuli. Clear waveforms were identified for all tone-burst frequencies for any of the SOA conditions from 1175 to 150 ms in the gap condition. The CAEP waveforms were characterized by a prominent N1. Conversely, in the non-gap condition, responses were identifiable at the 2 shortest SOAs conditions, only for the 3 tone-bursts with lowest frequencies. The low CAEP amplitudes in the non-gap condition suggest that high repetition of auditory stimulation reduces the firing response of auditory cortical cells. Thus, the low response amplitude may represent long-term adaptation probably caused by both synaptic depression (Asari and Zador, 2009, Wehr and Zador, 2005) and slow afterhyperpolarisation (Faber and Sah, 2003, Schwindt et al, 1988) in the absence of breaks, here for approximately 9 minutes (i.e. the duration of the sequence). The response morphology similarity in the gap condition between the waveforms elicited for the 150 and 250 ms SOAs to the 650 ms SOA (See Figure 5.B) suggests that the LS

deconvolution has been effective in reducing the response distortion resulting from multiple response overlaps.

Numerous studies have investigated neural adaption in the auditory cortex using the CAEP component as a marker (Herrmann et al, 2013, McEvoy et al, 1997, Rosburg et al, 2010). However, there is a significant lack of results for short SOA conditions where multiple responses overlap in time. The absence of results in this research area originates from the nonexistence of deconvolution techniques allowing the extraction of responses under low-jitter condition for multiple types stimuli. Importantly, previous research investigating CAEPs used rapidly presented stimulus sequences containing a high proportion of jitter, up to 900 ms (Budd and Michie, 1994, Loveless et al, 1989, Loveless et al, 1996). Findings of studies using ADJAR level 1 to correct for response overlap showed an enhancement of the N1 component for time intervals shorter than 400 ms (Budd and Michie, 1994, Wang et al, 2008a). A CAEP enhancement has also been reported for short SOAs jittered around 150 or 250 ms using the LS deconvolution in a paired paradigm (Bardy et al, 2014b).

The absence of response enhancement in the present study for short SOAs in the no-gap condition using sound sequence having a narrow jitter range reflects the importance of the temporal arrangement of the stimuli in the sound sequence on the CAEP amplitudes. Interestingly, the grand average waveform of the second stimulus of the gap condition for the ~150 ms SOA showed a larger P2 amplitude when compared to the ~250ms SOA. The enhanced response may have been due to the presence of a gap of 1600 ms every 6 stimuli. These results indicate that the neural adaptation in the auditory cortex may scale with the length of a sustained stimulation.

Frequency change of the tone-burst

In agreement with other studies, the experimental results showed a main effect of the tone-burst frequency with the high-frequency stimuli eliciting smaller cortical responses, and hence poorer SNRs, than lower-frequency (Jacobson et al, 1992, Picton et al, 1978).

One of the major advantages of the LS deconvolution technique is that it allows the recovery of sequences containing multiple different stimuli which can vary in spectral content. This has two practical benefits. First, changing the frequency of the stimuli is beneficial in reducing the amount of adaptation, hence allowing for larger responses (Herrmann et al, 2013). Second, such a paradigm allows the study of how the auditory system encodes more naturalistic sound sequences containing rapid spectral and temporal modulation.

Limitation of the deconvolution: Assumptions & SNR

The deconvolution makes two assumptions: 1) a constant morphology of responses within one particular jitter range; 2) auditory cortical responses to temporally close events add up linearly. However, these assumptions can be violated to varying degrees in real data. For example, CAEP variability during the entire recording, or morphology changes for different SOAs could violate the first assumption. Nevertheless, as mentioned previously, the assumption of a fixed CAEP shape with varying SOAs was made practically possible using low-jittered sequences. Concerning the second assumption, interactions between CAEP response and the non-linear superposition of different CAEP components could be a limitation. For example, it has been shown the N1 component has up to six generators (Näätänen and Picton, 1987). How components from different generator sites in the auditory cortex combine is unknown. Further work including the development of a non-linear version of the LS deconvolution as well as the recording of CAEPs using multi-electrode recordings and dipole source analysis to take in account the spatial component will be a next research step. These two assumptions were empirically validated by comparing the CAEPs in sequences S5 and S6 (SOA ~150+ Gap and SOA ~250 + Gap), which closely resemble the CAEP waveform morphology estimated using normal averaging (SOA~650 ms + Gap), but with a monotonic increase of the response amplitude with increasing SOA. We believe that the poor morphology of the responses recovered in sequences S1 and S2 (SOA ~150 ms and SOA ~250 ms) for the higher frequencies originated from the low SNRs for these recording conditions. As the SOA decreases, the CAEP tends

to diminish in size so that increasing the number of stimuli (i.e. in sequences S1 and S2) is not sufficient to maintain a certain "signal to noise ratio", and therefore leads to difficulties in interpreting the waveform morphology. The degree of accuracy of reconstruction using the LS deconvolution is dependent on the SNR of the recorded response as demonstrated in simulation by Bardy et al (2014a).

SNR: Adaptation of the response & noise introduced by the technique

Measurement times for each of the seven sequences were kept as constant as protocol design allowed. It made possible the presentation of more stimuli for the short SOA conditions (see Table 1) and consequently a *potential* noise reduction benefit which, if true, could be made use of by shortening the time for acquiring CAEPs.

There are two important conclusions. First, the SNR improvement when using the LS deconvolution technique in combination with high presentation rate stimulus sequences is affected by the numerical error introduced by the deconvolution (See figure 4.B and 6.B). Second, the potential SNR improvement using high presentation rates is counteracted by the decrease of the CAEP amplitude due to the adaptation associated with rapid presentation. Importantly, the results demonstrate that an SNR improvement cannot be achieved when using fast presentation rates (see Figure 6.C) due to the large response amplitude reduction for short SOA conditions. Therefore, based on the results, the LS deconvolution applied to CAEPs could not reduce measuring time and a significantly larger SNR was achieved for rates where conventional averaging was used (i.e. sequences S3, S4 and S7).

6. Conclusion

Simulations and real-life data showed that the LS deconvolution technique can reliably reconstruct multiple waveforms with low frequency content such as CAEP from different stimuli in a stimulus train, both with and without gaps between these trains. After optimization of high-rate stimulation sequences using low jitter, simulations showed that only a small SNR improvement is possible,

mainly due to the numerical error introduced by the mathematical inverse operation in the deconvolution. Moreover, this improvement was possible only in the absence of adaptation of the cortical response. Unfortunately, experimental CAEP recordings showed a large amplitude reduction with an increase in presentation rate. This suggests that sequences using high presentation rates cannot be used to improve the SNR of CAEP recordings. Nevertheless, such techniques could be applied to better understand the adaptation and morphology of the cortical responses to rapidly presented acoustic stimuli. This is particularly relevant as the brain generally encodes stimuli, like speech, that arrive at rates faster than once every second.

6.1 Further investigations

The development of the LS deconvolution technique was initiated in order to enable new experimental stimulus sequences. These have the potential to improve our understanding about how the brain is encoding and processing auditory stimuli arriving and changing at rapid rates which is an important function of the human auditory system.

Interestingly in this study, if the stimuli were presented without long gaps, the responses were largely reduced, as compared to conditions where a gap of 1600 ms was present every 6 stimuli. It suggests that the auditory cortex is attenuating its response to signals that are repetitive and continuous, so as not to waste its resources on signals that provide no new information. In contrast, the conditions including a gap, which correspond more closely to the temporal characteristics of running speech are more strongly encoded.

Establishing the validity of the use of the deconvolution in paradigms containing multiple events lays the foundation for further investigations into the use of CAEPs in response to closely spaced stimuli to evaluate temporal processing ability. In future designs, we can imagine the creation of stimulus sequences using the spectro-temporal characteristics of speech signals and thence deconvolution to analyze the data.

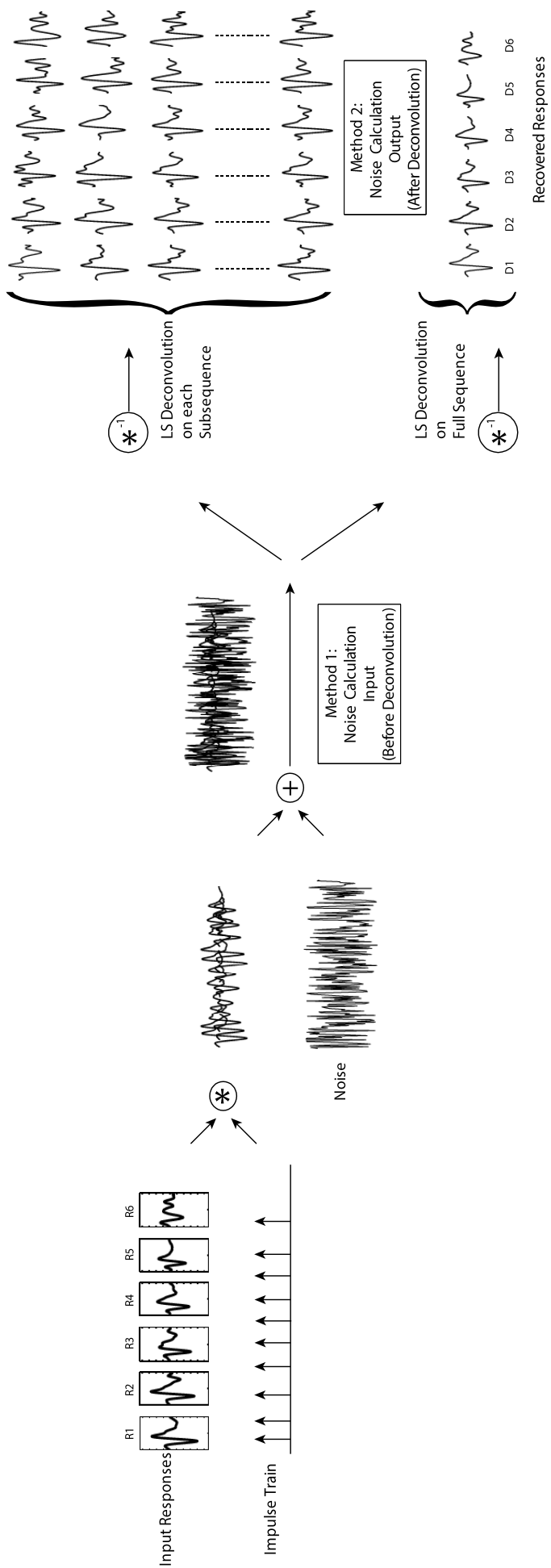**Acknowledgements**
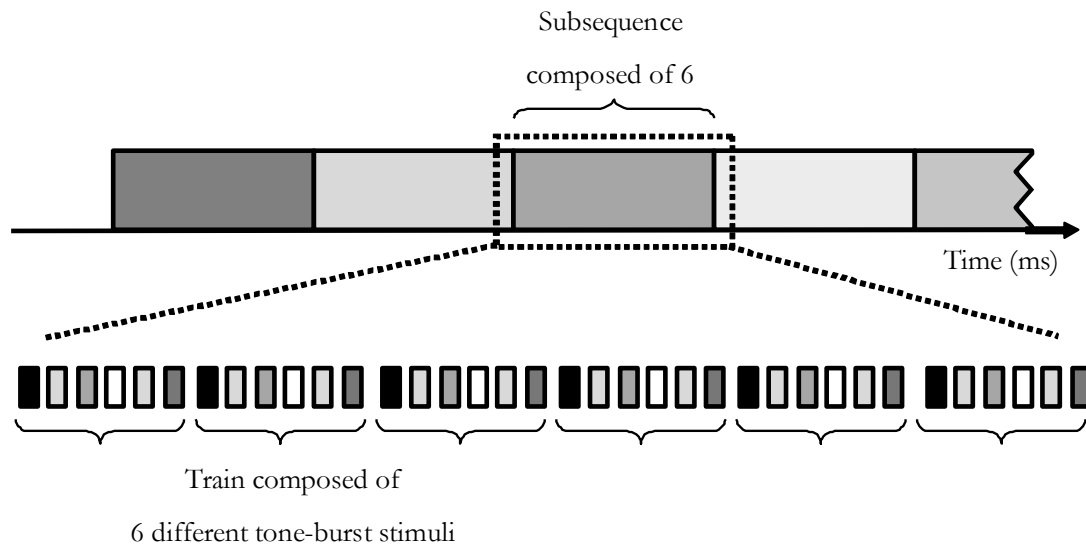
Figures

Figure 1. Schematic representation of a stimulus sequence in a multiple auditory stimuli paradigm. Each sequence is composed of an integer number of subsequences, themselves composed of six trains, each of six different tone-burst stimuli wi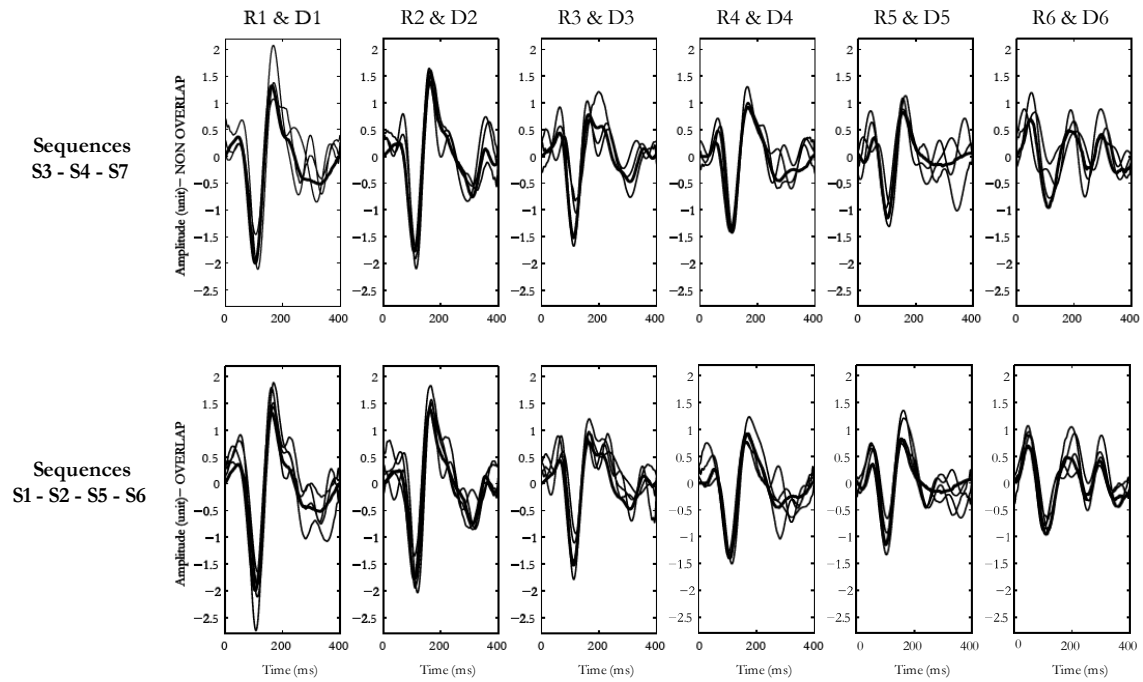th frequencies of 8, 4, 2, 1, 0.5, and 0.25 kHz. Consequently, each subsequence is composed of 36 stimuli. For sequences S1, S2 and S3, SOAs are jittered around 150, 250 and 650 ms respectively. In sequence S4, SOA is constant and equal to 1175 ms. Lastly, in sequences S5, S6 and S7, SOAs are jittered around 150, 250 and 650 ms respectively and a constant GAP interval of 1600 ms separates each stimulus train.
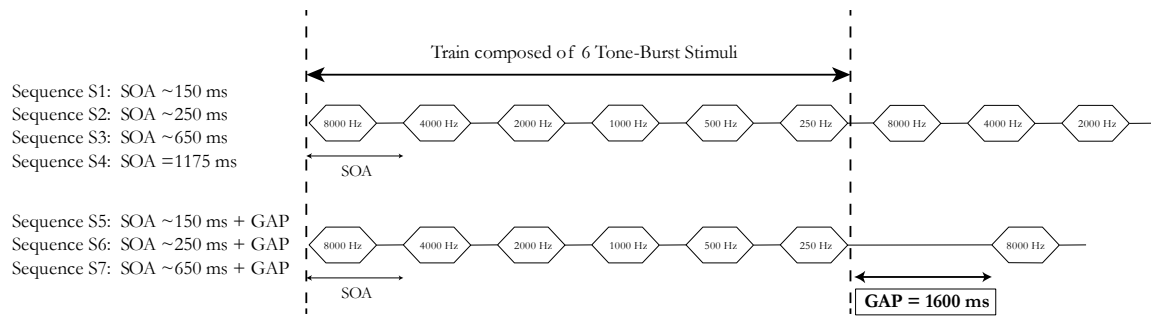
Figure 2. Schematic representation of the several processing stages of the simulations conducted using artificial data. The input signal is obtained by convolution of the impulse train of the stimulus sequences with six different artificial responses (annoted from R1 to R6). Additional noise is superimposed on the convolved responses before deconvolution. The LS deconvolution is performed both on each subsequence and on the full sequence. The noise is calculated both at the input of the simulation (before deconvolution), as well as the output of the simulation (after deconvolution). The quality of response recovery is evaluated by direct comparison of the recovered responses D1 to D6 with the original input responses R1 to R6.

Figure 4.3 Schematic representation of the several processing stages of the simulations conducted using artificial data. The input signal is obtained by convolution of the impulse train of the stimulus sequences with six different artificial responses (annoted from R1 to R6). Additional noise is superimposed on the convolved responses before deconvolution. The LS deconvolution is performed both on each subsequence and on the full sequence. The noise is calculated both at the input of the simulation (before deconvolution), as well as the output of the simulation (after deconvolution). The quality of response recovery is evaluated by direct comparison of the recovered responses D1 to D6 with the original input responses R1 to R6.
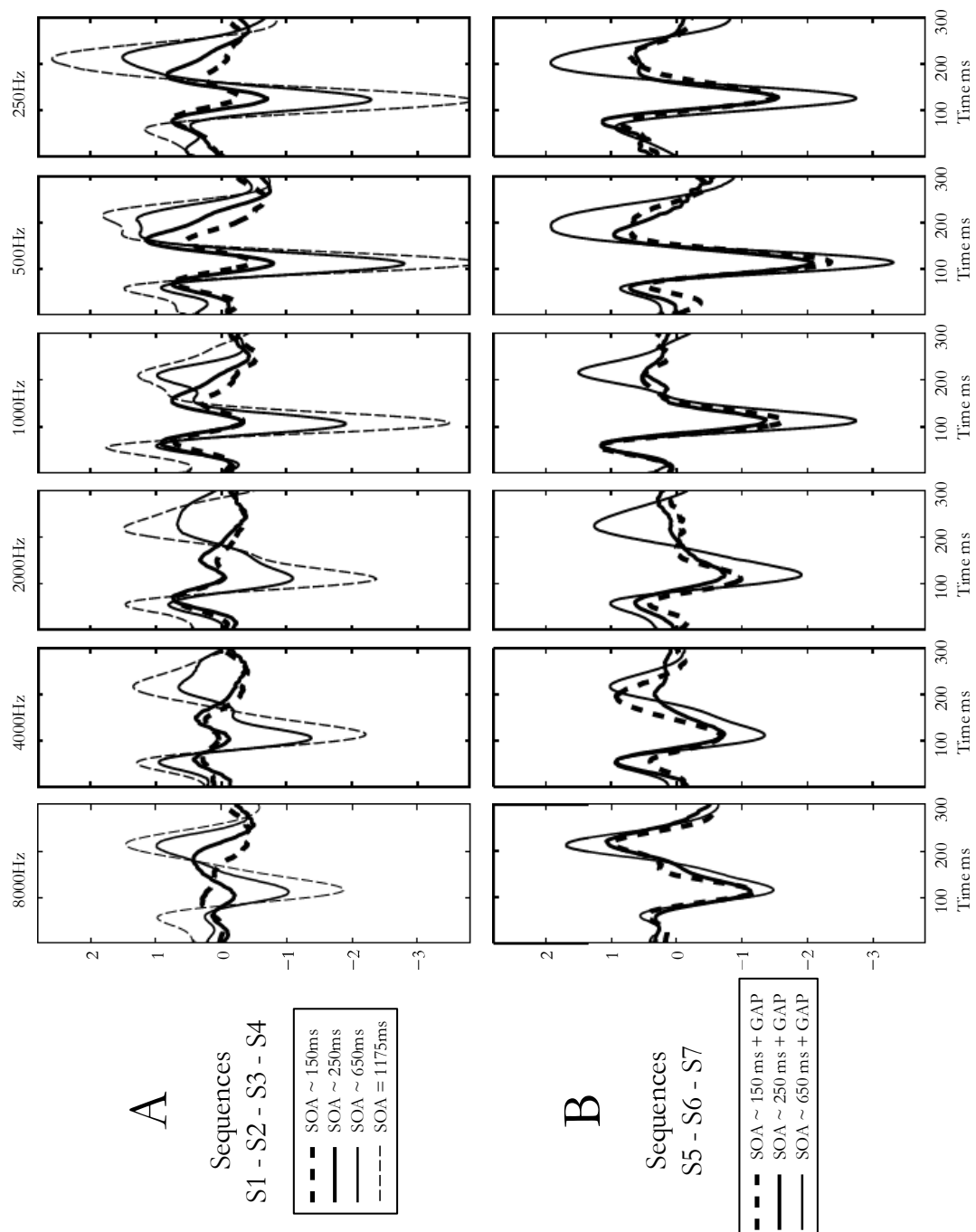
Figure 4. Results of the simulations for the 7 stimulus sequences. As shown, for calculation based on either the input waveforms (before deconvolution) or the output waveforms (after deconvolution): (A) input signal and output signal + noise power, (B) residual noise power, (C) SNR (in dB) of average powers, (D) ICC, represent a measure of similarity between input and output responses of the simulation.
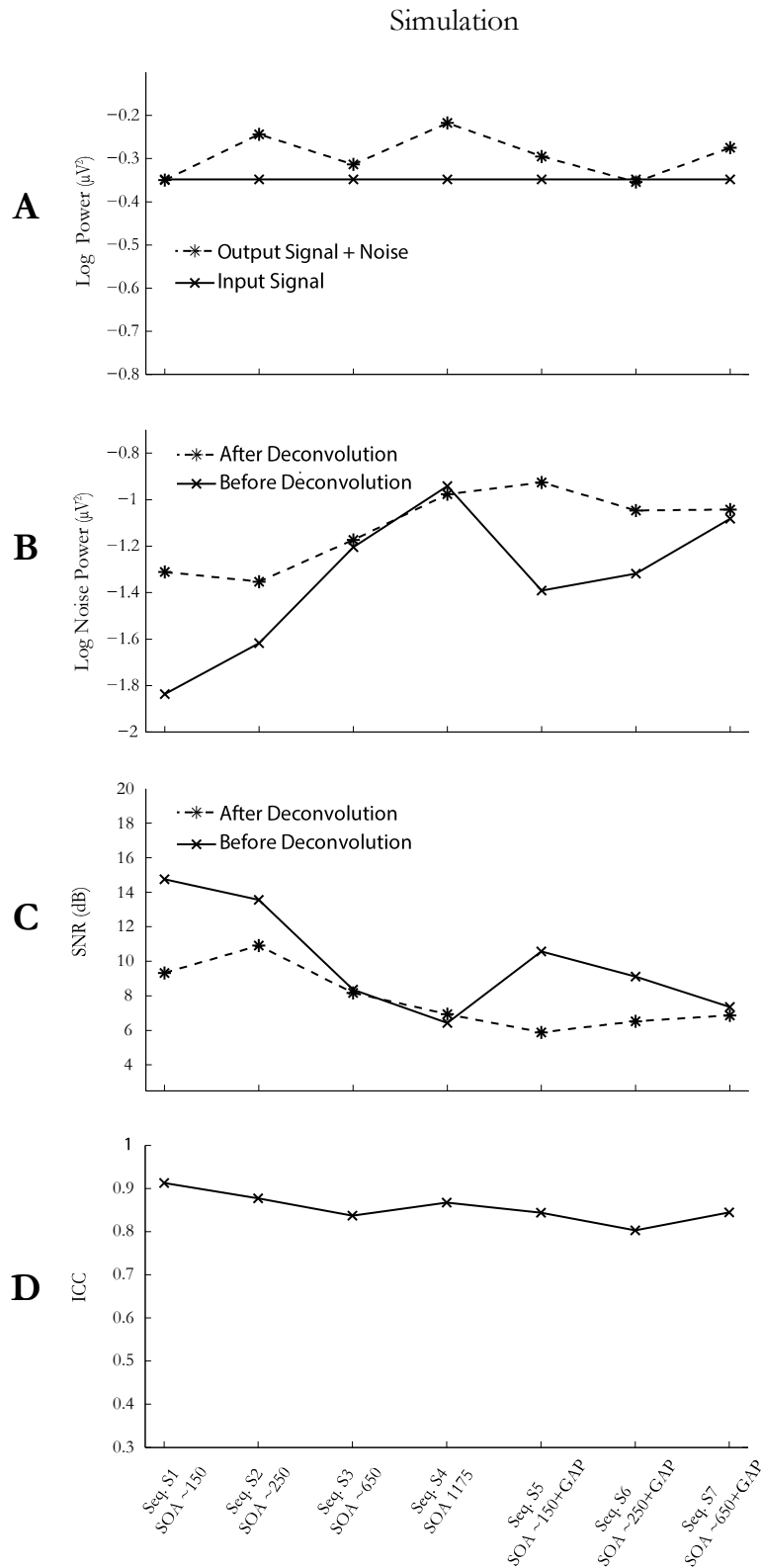
Figure 5. Grand average waveforms at different SOAs for (A) sequences S1 – S2 – S3 – S4, and (B) sequences S5 – S6 – S7 across 24 subjects for the 6 tone-burst stimuli with frequencies of 8, 4, 2, 1, 0.5, and 0.25 kHz.

Figure 6. Results of the experimental data for the 7 stimulus sequences. As shown, for calculations based on the input (before deconvolution) and output (after deconvolution): (A) signal plus noise power, (B) residual noise power, (C) SNR (in dB) of average powers for each participant. Vertical lines represent standard deviations between participants.
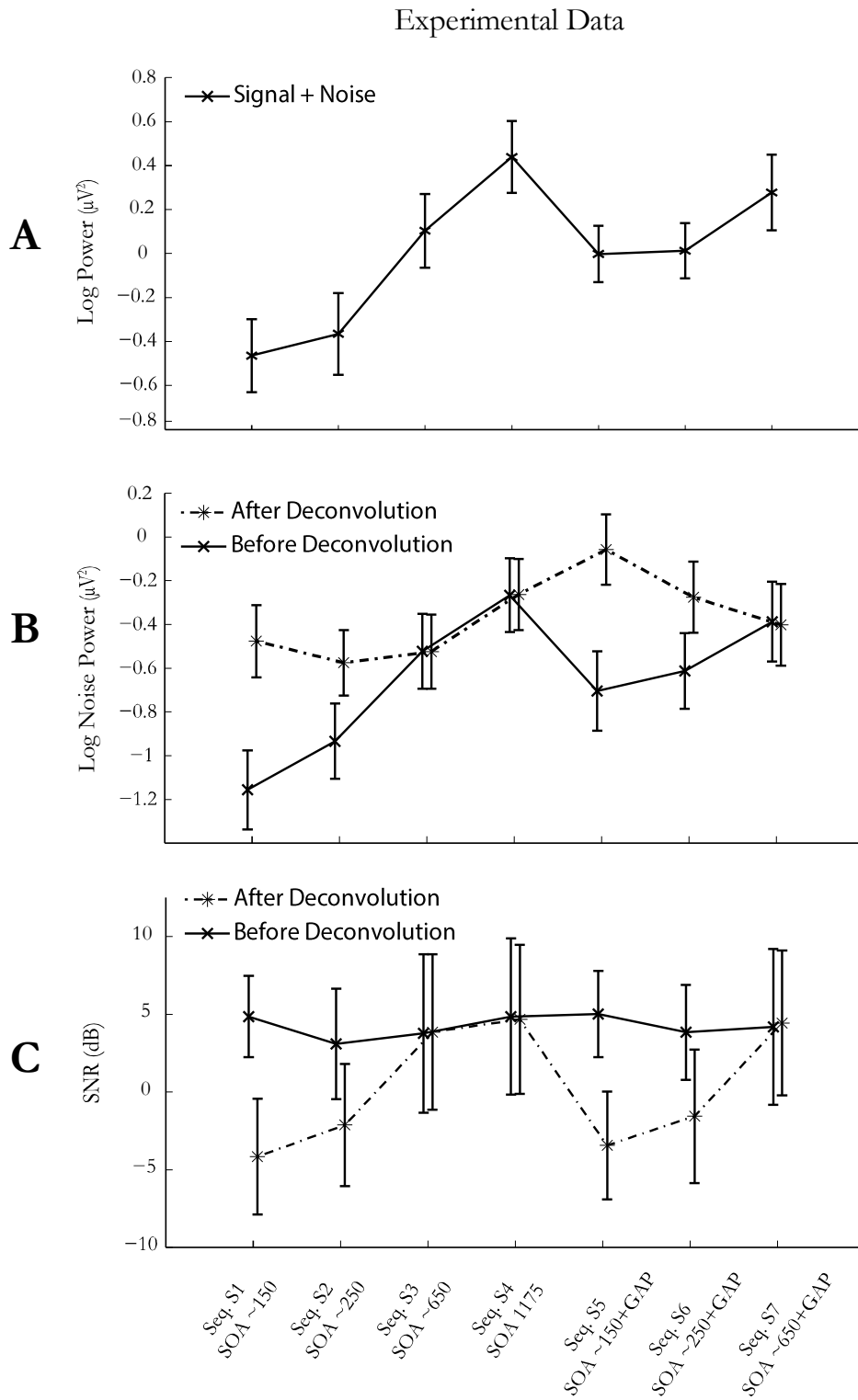
Figure 7. Signal power results for the 6 tone-burst stimuli with frequencies of 8, 4, 2, 1, 0.5, and 0.25 kHz, for the SOA jittered around 150, 250 and 650 ms. The solid lines depict the no-gap, while the dashed line depicts the gap condition. Vertical lines represent standard deviations.

Table

Sequence no	No GAP			Constant SOA	GAP of 1600 ms		
Sequence no	S1	S2	S3	S4	S5	S6	S7
SOA (ms) [jitter range]	150 [120-185]	250 [220-285]	650 [620-685]	1175	150 [120-185]	250 [220-285]	650 [620-685]
Nb subsequences	100	60	23	13	36	29	17
CN (simulation)	201.0	32.2	1.0	1.0	177.8	32.8	1.0
CN (exp. data) (SD)	212.8 (14.9)	42.2 (7.4)	1.0 (0.0)	1.0 (0.0)	182.5 (3.0)	33.5 (0.8)	1.0 (0.0)
Duration (min)	8.24	9.14	9.08	8.99	9.14	8.48	8.27

Table 1. Characteristics of the 7 stimulus sequences used for simulation and experimental recording. It shows the SOA range, the number of subsequences contained in each sequence, the condition number (CN) for the simulated, as well as for the experimental data (and their standard deviations), and the presentation duration of each of the 7 sequences. For the experimental data, the CN were given with with their respective standard deviations as the characteristic of the stimulus sequence was succeptible to change depending on the impact of the artefact rejection.

7. References

Asari H, Zador A M 2009 Long-lasting context dependence constrains neural encoding models in rodent auditory cortex *J. Neurophysiol.* **102** 2638-56

Bardy F, Dillon H, Van Dun B 2014a Least-squares deconvolution of evoked potentials and sequence optimization for multiple stimuli under low-jitter conditions *Clin. Neurophysiol.* **125** 727-37

Bardy F, Van Dun B, Dillon H, McMahon C M 2014b Deconvolution of overlapping cortical auditory evoked potentials (CAEPs) recorded using short stimulus onset-asynchrony (SOA) ranges *Clin. Neurophysiol.* **125** 814-26

Billings C J, Papesh M A, Penman T M, Baltzell L S, Gallun F J 2012 Clinical use of aided cortical auditory evoked potentials as a measure of physiological detection or physiological discrimination *Int. J. Otorhinolaryngol.* http://dx.doi.org/10.1155/2012/365752

Budd T W, Michie P T 1994 Facilitation of the N1 peak of the auditory ERP at short stimulus intervals *Neuroreport* **5** 2513-16

Cone B, Whitaker R 2013 Dynamics of infant cortical auditory evoked potentials (CAEPs) for tone and speech tokens *Int. J. Pediatr. Otorhinolaryngol.* **77** 1162-73

Delgado R E, Ozdamar O 2004 Deconvolution of evoked responses obtained at high stimulus rates *J. Acoust. Soc. Am.* **115** 1242-51

Delorme A, Makeig S 2003 EEGLAB: an open source toolbox for analysis of single-trial EEG dynamics including independent component analysis *J. Neurosci. Methods* **134** 9-21

Eysholdt U, Schreiner C 1982 Maximum length sequences - A fast method for measuring brain-stem-evoked responses *Int. J. Audiol.* **21** 242-50

Faber E L, Sah P 2003 Calcium-activated potassium channels: multiple contributions to neuronal function *Neuroscientist* **9** 181-94

Fox A M, Anderson M, Reid R, Smith T, Bishop D M V 2010 Maturation of auditory temporal integration and inhibition assessed with event-related potentials (ERPs). *BMC Neurosci.* **11** 1471-2202

Golding M, Pearce W, Seymour J, Cooper A, Ching T, Dillon H 2007 The relationship between obligatory cortical auditory evoked potentials (CAEPs) and functional measures in young infants *J. Am. Acad. Audiol.* **18** 117-25

Golding M, Purdy S C, Sharma M a, Dillon H 2006 The effect of stimulus duration and inter-stimulus interval on cortical responses in infants *Aust N Z J Audiol* **28** 122-36

Herrmann B, Henry M J, Obleser J 2013 Frequency-specific adaptation in human auditory cortex depends on the spectral variance in the acoustic stimulation *J. Neurophysiol.* **109** 2086-96

Jacobson G P P, Lombardi D M M A, Gibbens N D M A, Ahmad B K M, Newman C W P 1992 The effects of stimulus frequency and recording site on the amplitude and latency of multichannel cortical auditory evoked potential (CAEP) component N1 *Ear Hear.* **13** 300-06

Jewett D L, Caplovitz G, Baird B, Trumpis M, Olson M P, Larson-Prior L J 2004 The use of QSD (q-sequence deconvolution) to recover superposed, transient evoked-responses *Clin. Neurophysiol.* **115** 2754-75

Loveless N, Hari R, Tiihonen J 1989 Evoked responses of human auditory cortex may be enhanced by preceding stimuli *Electroencephalogr. Clin. Neurophysiol.* **74** 217-27

Loveless N, Levänen S, Jousmäki V, Sams M, Hari R 1996 Temporal integration in auditory sensory memory: neuromagnetic evidence *Electroencephalogr. Clin. Neurophysiol.* **100** 220-28

McEvoy L, Levanen S, Loveless N 1997 Temporal characteristics of auditory sensory memory: neuromagnetic evidence *Psychophysiol.* **34** 308-16

McGraw K O, Wong S 1996 Forming inferences about some intraclass correlation coefficients *Psychol. Methods* **1** 30

Mou-yan Z, Unbehauen R 1995 On the computational model of a kind of deconvolution problem *IEEE Trans. Image. Process.* **4** 1464-67

Näätänen R, Picton T W 1987 The N1 wave of the human electric and magnetic response to sound: A review and an analysis of the component structure *Psychophysiol.* **24** 375-425

Onishi S, Davis S 1968 Effects of duration and rise time of tone bursts on evoked V potentials *J. Acoust. Soc. Am.* **44** 582-90

Oxenham A J, Plack C J 1998 Suppression and the upward spread of masking *J. Acoust. Soc. Am.* **104** 3500-10

Ozdamar O, Bohorquez J 2006 Signal-to-noise ratio and frequency analysis of continuous loop averaging deconvolution (CLAD) of overlapping evoked potentials *J. Acoust. Soc. Am.* **119** 429-38

Picton T W, Woods D L, Proulx G B 1978 Human auditory sustained potentials. II. Stimulus relationships *Electroencephalogr. Clin. Neurophysiol.* **45** 198-210

Rance G, Cone-Wesson B, Wunderlich J, Dowell R 2002 Speech perception and cortical event related potentials in children with auditory neuropathy *Ear Hear.* **23** 239

Rosburg T, Zimmerer K, Huonker R 2010 Short-term habituation of auditory evoked potential and neuromagnetic field components in dependence of the interstimulus interval *Exp. Brain Res.* **205** 559-70

Sable J, Low K, Maclin E, Fabiani M, Gratton G 2004 Latent inhibition mediates N1 attenuation to repeating sounds *Psychophysiol.* **41** 636-42

Schwindt P, Spain W, Foehring R, Stafstrom C, Chubb M, Crill W 1988 Multiple potassium conductances and their functions in neurons from cat sensorimotor cortex in vitro *J. Neurophysiol.* **59** 424-49

Sharma A, Gilley P M, Dorman M F, Baldwin R 2007 Deprivation-induced cortical reorganization in children with cochlear implants *Int. J. Audiol.* **46** 494-99

Souza P E, Tremblay K L 2006 New perspectives on assessing amplification effects *Trends In Amplif.* **10** 119-43

Stapells D R 2002 Cortical Event-Related Potentials to Auditory Stimuli In Katz J, Handbook of Clinical Audiology (5th ed Philadelphia, USA: Lippincott Williams & Wilkins) p 378-405

Sussman E, Steinschneider M, Gumenyuk V, Grushko J, Lawson K 2008 The maturation of human evoked brain potentials to sounds presented at different stimulus rates *Hear. Res.* **236** 61-79

Valderrama J T, Alvarez I, de la Torre A, Carlos Segura J, Sainz M, Luis Vargas J 2012 Recording of auditory brainstem response at high stimulation rates using randomized stimulation and averaging *J. Acoust. Soc. Am.* **132** 3856-65

Van Dun B, Carter L, Dillon H 2012 Sensitivity of cortical auditory evoked potential detection for hearing-impaired infants in response to short speech sounds *Audiol. Res.* **2** e13, 65-76

Wang A, Mouraux A, Liang M, Iannetti G 2008a The enhancement of the N1 wave elicited by sensory stimuli presented at very short inter-stimulus intervals is a general feature across sensory systems *PLoS ONE* **3** e3929

Wang T, Jiang-Hua H, Lin L, Zhan C a A 2013a Continuous-and Discrete-Time Stimulus Sequences for High Stimulus Rate Paradigm in Evoked Potential Studies *Comput. Math. Methods Med.* **2013**

Wang T, Su Y Y, Shen Q, Ma J 2008b A simulation study assessing the efficiency of deriving evoked responses using high stimulus rate In: 30th Annual International Conference of Engineering in Medicine and Biology Society (EMBS). Vancouver: IEEE; p. 5033-36.

Wang T, Zhan C, Yan G, Bohórquez J, Özdamar Ö 2013b A preliminary investigation of the deconvolution of auditory evoked potentials using a session jittering paradigm *J. Neural Eng.* **10** 026023

Wehr M, Zador A M 2005 Synaptic mechanisms of forward suppression in rat auditory cortex *Neuron* **47** 437-45

Yamashiro K, Inui K, Otsuru N, Kakigi R 2011 Change-related responses in the human auditory cortex: An MEG study *Psychophysiol.* **48** 23-30

Zacharias N, Sielużycki C, Kordecki W, König R, Heil P 2011 The M100 component of evoked magnetic fields differs by scaling factors: Implications for signal averaging *Psychophysiology* **48** 1069-82